Thin Solid Films 528 (2013) 67–71

Contents lists available at SciVerse ScienceDirect

Thin Solid Films

journal homepage: www.elsevier.com/locate/tsf

Effect of thermal treatment on physical, electrical properties and reliability of porogen-containing and porogen-free ultralow-*k* dielectrics

Yu-Min Chang [a], Wei-Yuan Chang [b], Jun-Fu Huang [b], Jihperng Leu [a], Yi-Lung Cheng [b,*]

[a] Department of Material Science and Engineering, National Chiao-Tung University, Shin-Chu, Taiwan, ROC
[b] Department of Electrical Engineering, National Chi-Nan University, Nan-Tou, Taiwan, ROC

ARTICLE INFO

Available online 6 November 2012

Keywords:
Low-*k* dielectric
Porogen
UV curing
Reliability
Breakdown
TDDB

ABSTRACT

The effects of thermal annealing on the physical, electrical properties and reliability of porogen-containing and porogen-free ultralow-*k* dielectrics prepared by plasma-enhanced chemical vapor deposition (PECVD) are investigated. The porogen-free low-*k* dielectrics are obtained by using UV curing process to removal organic sacrificial phase and to generate open porosity. The results are compared with PECVD porogen-containing low-*k* films fabricated without UV curing process and PECVD low-*k* dielectrics deposited without organic sacrificial phase. The experimental results show that all low-*k* films remained stable after they were experimentally heating to temperatures up to 700 °C. The non-porous low-*k* films also showed the highest reliability. Although the porous-free low-*k* film requires an additional UV curing process, the heat stress confirmed that its thermal stability was better than that of the porogen-containing low-*k* film. At an annealing temperature above 500 °C, the heating process is comparable to UV curing, but does not provide Si–O–Si cross-linking within the film. At an annealing of 600 °C, the porogen-free low-*k* films have a relatively higher breakdown electric-field and longer failure time in comparison to the porogen-containing low-*k* films. However, pores generated in porogen-containing low-*k* films at high temperature cause reliability to degrade with annealing temperature.
Crown Copyright © 2012 Published by Elsevier B.V. All rights reserved.

1. Introduction

Advanced Cu/low-*k* integration interconnects the use of porous organosilica low-*k* materials with *k*-values between 2.4 and 3.0 to reduce signal propagation delay, cross-talk, and power consumption in integrated circuit [1–3]. A major strategy for decreasing the *k*-value of dielectric films is introducing the material porosity [4,5]. Recently, microelectronic applications of PECVD low-*k* films have increased due to their simplicity and compatibility with technology requirements [6]. Porosity is introduced into PECVD low-*k* dielectric mainly by using sacrificial porogens [7], which are cyclic hydrocarbons that can be removed by UV-assisted-thermal curing [8]. The porogen molecules are photodissociated by UV light with the formation of volatile hydrocarbons and nonvolatile carbon-rich porogen residues [9].

During the interconnect fabrication process and IC packaging step, thermal annealing process is the indispensable step [10–12]. Additionally, annealing of lower level interconnects is performed many times higher than those for annealing of upper level interconnects when fabricating multilevel interconnects. Therefore, the effects of thermal annealing process on the film properties of porous low-*k* materials should be addressed. Moreover, the effects of thermal annealing on the interconnect performance, particularly reliability, must also be considered. Consequently, the main purpose of this work is to clarify the stability of various low-*k* materials, including non-porous and porous materials, when exposed to heat stress. Basic film properties, porosity, mechanical, and electrical performance were performed to clarify how thermal stress affects the chemical structure of dielectric films. Finally, the intrinsic reliability of TDDB results for the low-*k* dielectrics under the different thermal stresses was also investigated.

2. Experiments

All thin film depositions were performed on 300 mm p-type Si wafers by Applied Material PECVD reactor with a radio frequency (rf) of 13.56 MHz at a temperature of 300 °C. Three different low-*k* films with approximate thicknesses of 300 nm were obtained in this study. The porogen-containing low-*k* films were deposited from diethoxymethylsilane (DEMS) and alpha-terpiene (ATRP) as a matrix and porogen precursor, respectively. A small amount of oxygen was also introduced as an oxidant. To create the porogen-free low-*k* films, UV curing of the porogen-containing low-*k* films was performed to remove the organic porogen for 10 min. The low-*k* films deposited without organic porogen content (briefly call "low-*k* without porogen) were also prepared in the same system as a reference. All low-*k* films were thermally annealed at varying temperatures (400–900 °C) in ambient N_2 for 1 min.

The thickness and refractive index (RI, at 633 nm) of the as-deposited films were analyzed with an ellipsometer in an optical-probe system. The film thickness shrinkage ratio was calculated as the difference in the film

* Corresponding author. Tel.: +886 49 2910960 4987; fax: +886 49 2917810.
E-mail address: yjcheng@ncnu.edu.tw (Y.-L. Cheng).

0040-6090/$ – see front matter. Crown Copyright © 2012 Published by Elsevier B.V. All rights reserved.
http://dx.doi.org/10.1016/j.tsf.2012.09.088

thickness before and after annealing process. Chemical bonding of the low-*k* films was characterized by Fourier transform infrared absorption (FTIR). A water contact angle tool was used to determine the hydrophilic/hydrophobic properties of the surface. Ellipsometric porosimetry (EP) was used to assess the isotherm of ethanol adsorption and desorption to determine the total porosity and the pore size. The nano-hardness and modulus of low-*k* films were measured on an MTS Nano Indentor XP system. The sample thickness for nano-hardness measurements was approximately 0.6 μm and the depth penetration was about 100 nm at down force of ~0.3 mN. The dielectric constant was obtained by measuring the capacitance–voltage using a mercury probe at 1 MHz. The metal–insulator–semiconductor (Al/low-*k*/Si; MIS) capacitors with p-type silicon (Si) as the substrates and aluminum (Al) as the metal electrodes were fabricated. The capacitors had an area of 30×30 μm^2. Negative voltages from 0 to 200 V were applied to the Al electrodes, and leakage–voltage (*I*–*V*) characteristics and dielectric breakdown electric fields were measured with a semiconductor analyzer (HP4286) at room temperature. Time-dependent dielectric breakdown (TDDB) measurements were performed on the same MIS capacitors.

3. Results and discussion

Fig. 1 shows the varying thickness shrinkage ratios and refractive index obtained for different low-*k* films at varying annealing temperatures from 400 °C to 900 °C. At annealing temperature above 800 °C, thickness decreased and refractive index significantly increased in all low-*k* films, which indicated that the low-*k* films analyzed here are thermally stable up to 700 °C. The porogen-containing low-*k* films without UV curing showed the largest declines in film thickness, especially at annealing temperatures above 500 °C. The reduced film thickness resulted mainly from the porogen decomposition, which implies that thermal treatment at an annealing temperature above 500 °C has a decomposing effect, similar to that of UV curing. The similar changes in the refractive index also demonstrate that the porogen materials in low-*k* films begin decomposing at annealing temperature above 500 °C. Compared to porogen-containing and porogen-free low-*k* films, the experiments showed that low-*k* films deposited without organic porogen content remain unchanged until the annealing temperature reaches 800 °C.

Fig. 2 compares the FTIR spectrum of the as-deposited low-*k* films. The characteristic absorptions are: network Si–O–Si stretching (~1060 cm^{-1}), cage-like Si–O–Si stretching (~1150 cm^{-1}), Si–O–Si bending (~440 cm^{-1}), $Si-CH_3$ bending (~1270 cm^{-1}), and $C-H_x$ stretching (~2850–3100 cm^{-1}). The figure shows that the porogen-

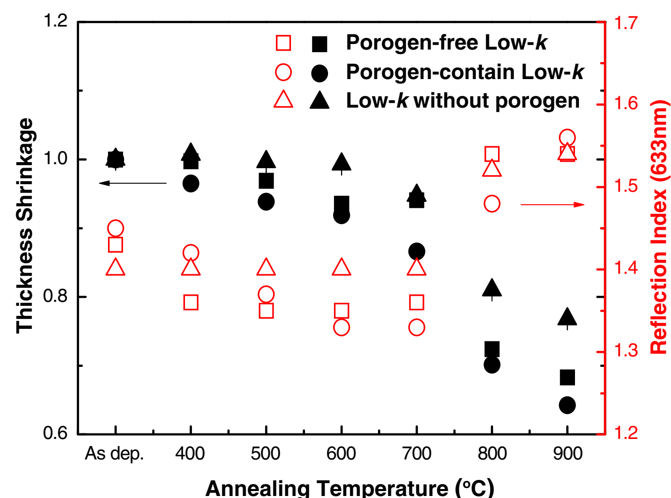

Fig. 1. Thickness shrinkage and refractive index as functions of annealing temperature for various low-*k* films.

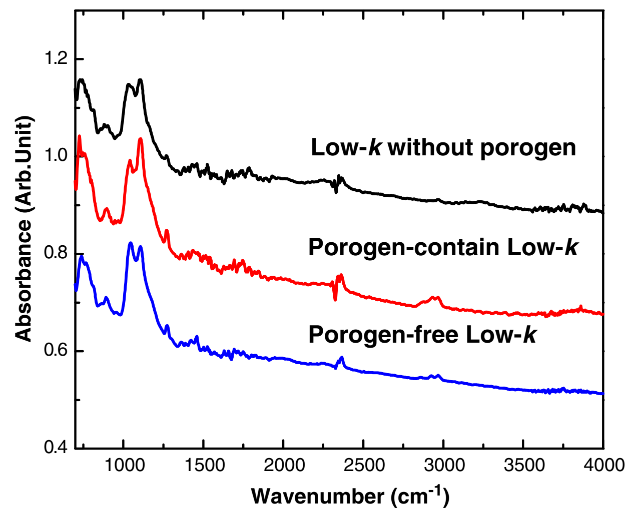

Fig. 2. FTIR spectra of as-deposited low-*k* films.

containing low-*k* film contains more $C-H_x$ stretching bonding, which indicates that this bonding is caused mainly by molecular porogen. To examine the effect of annealing temperature on the change in bonding structures, the relative area ratio of $Si-CH_3$ and $C-H_x$ bonds were analyzed as a function of annealing temperature. The relative area ratios are calculated from the following wavenumber regions:

$$\text{The}(Si-CH_3/Si-O)\text{peak ratio} = (1250\text{–}1285\,cm^{-1})/(950\text{–}1250\,cm^{-1}).$$

$$\text{The}(C-H_x/Si-O)\text{peak ratio} = (2800\text{–}3050\,cm^{-1})/(950\text{–}1250\,cm^{-1}).$$

Fig. 3 displays the analytical results. Comparison of the as-deposited low-*k* films shows that the low-*k* films deposited with organic porogen have higher ratios of $Si-CH_3$ and $C-H_x$ bonds in comparison to those without organic porogen. After 500 °C annealing, the ratio of $C-H_x$ bonding remains constant for all three low-*k* films. These experimental results also confirm that molecular porogen can be completely removed by annealing at a temperature above 500 °C. Analysis of $Si-CH_3$ bonding ratio shows that the porogen-free low-*k* film contains more $Si-CH_3$ bonds, which suggests that $Si-CH_3$ bonding can be created by UV irradiation. The same phenomenon was reported earlier in Choi et al. [10]. Additionally, $Si-CH_3$ bonding slightly declines at an annealing temperature of 700 °C and is completely eliminated at an annealing temperature of 900 °C. Further analysis of the −OH stretching mode in the

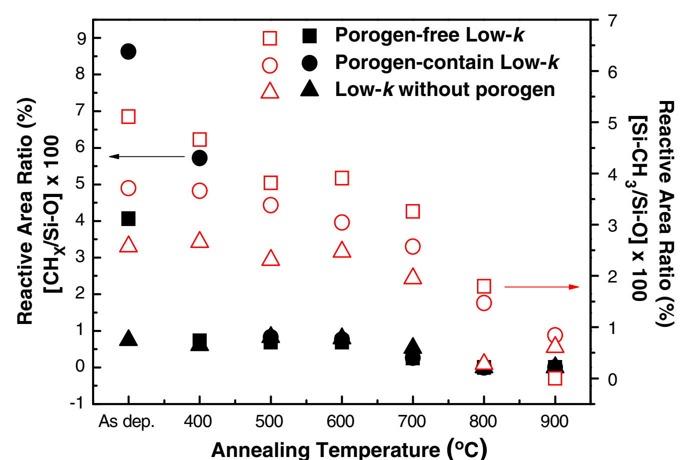

Fig. 3. FTIR ratios of $Si-CH_3/Si-O$ and $C-H_x/Si-O$ bonds as functions of annealing temperature for various low-*k* films.

3400 cm^{-1} region of the FTIR spectrum for all low-*k* films at thermal annealing temperature above 700 °C showed that −OH stretching mode correlates with annealing temperature. The formation of the −OH stretching mode can be explained as follows: Si−CH_3 bonds break to form Si· center dangling defect under thermal annealing at a temperature above 700 °C. These broken bonds can easily interact with OH/H_2O,

To understand the effect of annealing temperature on the hydrophilicity/hydrophobicity of the low-*k* films, water contact angle (WCA) was measured on the film surfaces. It is reported that the surfaces remained hydrophobic as WCA was higher than 85 °C [11]. Fig. 4 presents the WCA plot as a function of annealing temperature for various low-*k* films. Interestingly, comparison of three different low-*k* films shows that the porogen-free low-*k* film has the highest WCA, which indicates that this film is the most hydrophobic, possibly because the high ratio of Si−CH_3 bonds decreases the polarity required for the hydrophobic properties to the low-*k* material. The WCA is lowest in the low-*k* films deposited without porogen and its dependence on the annealing temperature is negligible, which suggests that the thermal annealing process does not change surface polarity. In the porogen-containing low-*k* films, WCA significantly increases when annealing temperature exceeds 500 °C, indicating that the porogen low-*k* films become more hydrophobic as the porogen was removed to form pores. This experimental result also implies that the internal pore surfaces of the films are hydrophobic. At annealing temperatures above 700 °C, WCA begins to decline in both low-*k* films deposited with porogen due to the formation of −OH bonds.

Fig. 5(a) and (b) shows the hardness (H) and elastic modulus (E), respectively, as functions of annealing temperature for the various low-*k* films. To avoid the substrate effect on the low-*k* films, the films with thicknesses greater than 600 nm was used for the nanoindentation measurements. The order of the as-deposited low-*k* films in terms of hardness and elastic modulus was: low-*k* films without porogen > porogen-free low-*k* films > porogen-containing low-*k* films. This order indicates that porogen degrades mechanical strength in the low-*k* film as reported in the literature [13]. Additionally, the UV curing process strengthens film bonding in porogen low-*k* films. Regarding the annealing temperature effect, annealing temperatures below 600 °C do not affect low-*k* films without organic porogen content. However, the mechanical strength of porogen-free and porogen-containing low-*k* films slightly decreases with annealing temperature, which indicates that thermal annealing alters the microstructure of porogen low-*k* films. Additionally, at annealing temperatures exceeding 700 °C, the elastic modulus and hardness begin to increase substantially in all low-*k* films. This improvement is attributable to changes in the bonding structure of the low-*k* films. FTIR analysis also shows that breaking the terminal Si−CH_3 and Si−H bonds in the low-*k* films causes formation of new Si−O−Si cross-linking bonds, which increases mechanical strength.

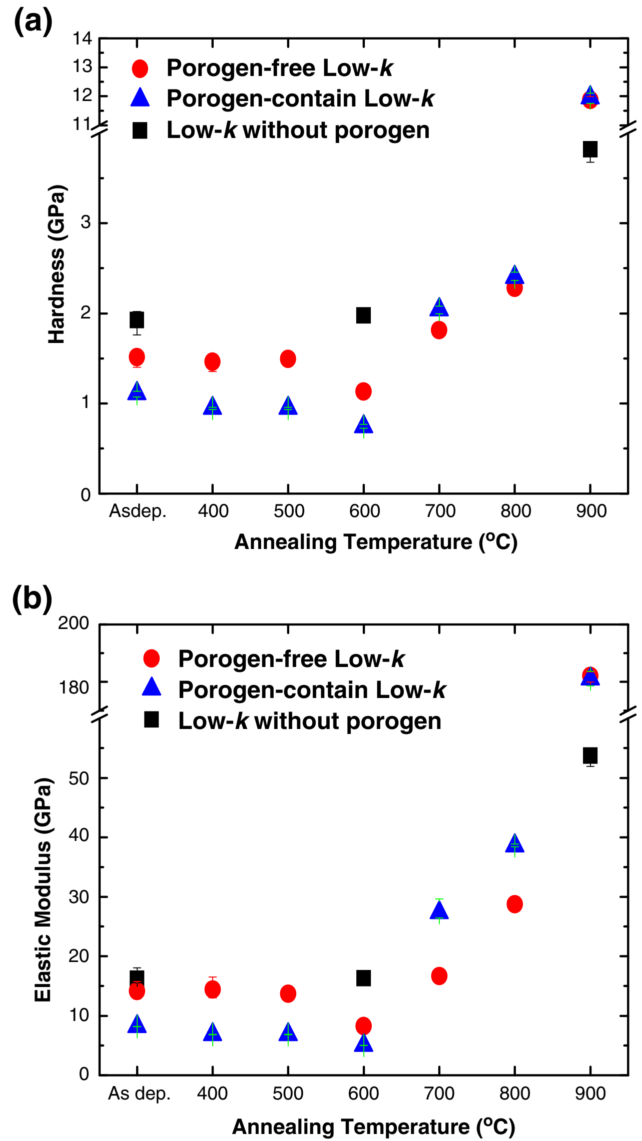

Fig. 5. (a) Hardness values as functions of annealing temperature and (b) elastic modulus as functions of annealing temperature for various low-*k* films.

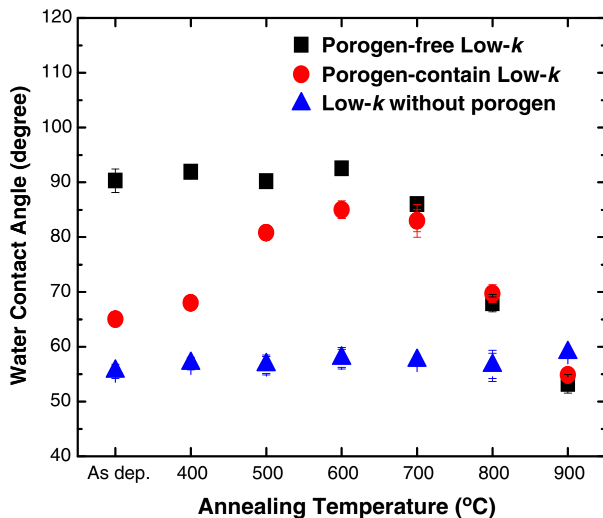

Fig. 4. Water contact angle value as functions of annealing temperature for various low-*k* films.

Table 1 presents the measured dielectric constant, pore size, and porosity of various low-*k* dielectrics at annealing temperatures of 400 °C and 600 °C. The data show that the porosity of the low-*k* film deposited without organic sacrificial phase approaches zero after the annealing process, which is consistent with the results of the thickness shrinkage and FTIR. This indicates that the low-*k* film deposited without organic sacrificial phase is thermally stable. In the porogen-free and porogen-containing low-*k* films without thermal annealing, the porosity of the porogen-free low-*k* film is about two-fold higher than that of the porogen-containing low-*k* film, which indicates that UV curing removes the organic sacrificial phase to produce pores in the low-*k* films. In the porogen-free low-*k* films, the porosity was unrelated to annealing temperature. In contrast, the porosity of the porogen-containing low-*k* film slightly increases after 400 °C annealing and significantly increases after 600 °C annealing. In low-*k* dielectrics annealed at 600 °C, the porosity of the porogen-containing low-*k* film is about 6% higher than that of the porogen-free

Table 1
Dielectric constant, porosity, and pore size for three different low-*k* films under various annealing temperatures.

Sample	As-deposited			400 °C annealed			600 °C annealed		
	Dielectric constant (k)	Porosity (%)	Pore size (nm)	Dielectric constant (k)	Porosity (%)	Pore size (nm)	Dielectric constant (k)	Porosity (%)	Pore size (nm)
Porogen-free low-*k*	2.42	13.4	1.35	2.36	14.1	1.35	2.05	15.3	1.7
Porogen-containing low-*k*	2.93	4.8	N/D	2.72	5.6	N/D	2.03	21.5	1.7
Low-*k* without porogen	3.0	N/D	N/D	2.9	N/D	N/D	2.93	N/D	N/D

N/D = not detected.

low-*k* film, which suggests that the porogen-free low-*k* film with UV curing strengthens some unstable bonds, which leads to a reduced porosity.

Fig. 6 shows the measured *k*-values of various low-*k* films at 1 MHz. The *k*-value of the as-deposited porogen-containing low-*k* films is approximately 2.9 due to their low open porosity. The UV curing reduces the *k*-value of porogen-free low-*k* film to about 2.4 due to partial porogen removal, resulting in the increased porosity of the film. Analysis of the annealing temperature effect shows that all low-*k* films significantly degrade at annealing temperature above 800 °C, which is consistent with the results of thickness shrinkage and FTIR. At annealing temperature below 800 °C, different low-*k* films display different temperature-dependence trends. In low-*k* films deposited without porogen, the *k*-values remain virtually unchanged. However, the *k*-values of low-*k* films deposited with porogen correlate negatively with annealing temperature. The decrease in the porogen-containing low-*k* films is larger than that in porogen-free low-*k* films. The decrease in the *k* value with the annealing temperature in the porogen-free low-*k* films suggests that UV curing did not completely remove molecular porogen and that the thermal process further decomposes the remaining porogen residues. This postulation is also supported by FTIR results, which show that the peak area of CH_x bonding decreases with annealing temperature.

Fig. 7 compares the *I*–*V* characteristics of MIS structures with different as-deposited low-*k* dielectrics. All low-*k* films show similar curves for leakage current density versus electrical-filed. The leakage current increases with the electrical filed before reaching a plateau. Finally, the leakage current density abruptly increases. Interestingly, the low-*k* films deposited without porogen have a higher leakage current, but a higher dielectric breakdown electric-field in comparison to the low-*k* films deposited with porogen. In the low-*k* films deposited with porogen, leakage current densities are comparable, but the porogen-free low-*k* films have a lower dielectric breakdown electric-field. These comparison results suggest that leakage current in low-*k* films seems to be impacted by the bonding structure and is not substantially impacted by porosity. However, porosity in the low-*k* film can affect dielectric breakdown strength. Fig. 8(a) and (b) compares the leakage current densities for electrical fields at 1 and 2 MV/cm and dielectric breakdown electric-field, respectively, as a function of annealing temperature. The leakage current densities significantly decrease with annealing process in the low-*k* films deposited without porogen, possibly due to moisture desorption. However, the dielectric breakdown electric-field is unaffected. In the porogen-containing low-*k* films, pore formation at annealing temperature of 600 °C slightly increases leakage current and substantially degrades the dielectric breakdown electric-field.

Time-dependence-dielectric-breakdown (TDDB) was also evaluated for various low-*k* dielectrics. Fig. 9(a) shows the failure time of the as-deposited low-*k* films versus electrical field for three different low-*k* dielectrics. This reliability assessment result shows a similar trend of degrading electrical properties in the low-*k* films deposited with porogen. Moreover, the porogen-free low-*k* films have a loner breakdown failure time compared to the porogen-containing low-*k* films. Fig. 9(b) compares the failure time at 63.2% failure rate with annealing temperature for three different low-*k* films. The electrical filed was increased (8.5 MV/cm) to stress the low-*k* films deposited without porogen in order to shorten the testing time. In the low-*k* films deposited without porogen, the failure times at a 63.2% failure rate are independent of annealing temperature, as observed in analyses of the dielectric breakdown electric-field. In the case of the low-*k* films deposited with porogen, annealing temperature affected dielectric breakdown failure time. However, the porogen-free and porogen-containing low-*k* films have a different temperature-dependence trend. In the porogen-containing low-*k* films, dielectric breakdown failure time correlates negatively with annealing temperature. In contrast, the dielectric breakdown failure time in the porogen-free low-*k* films increases when the

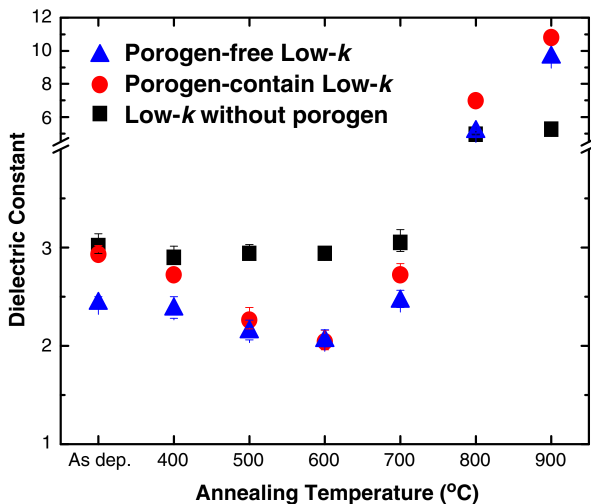

Fig. 6. Dielectric constants as functions of annealing temperature for various low-*k* films.

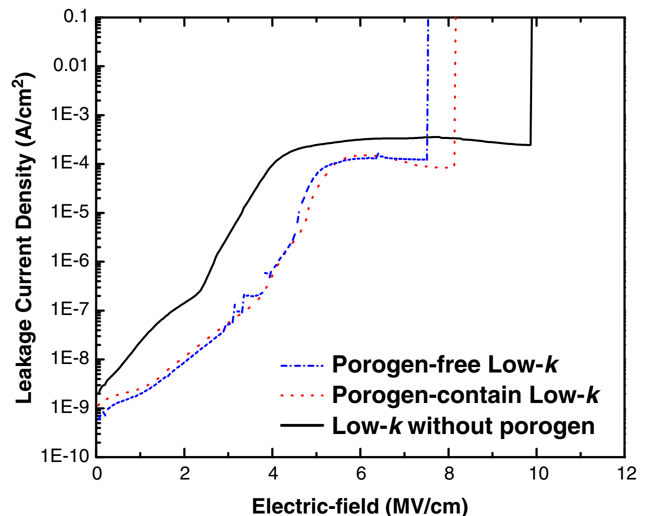

Fig. 7. *I*–*V* characteristics of as-deposited low-*k* films.

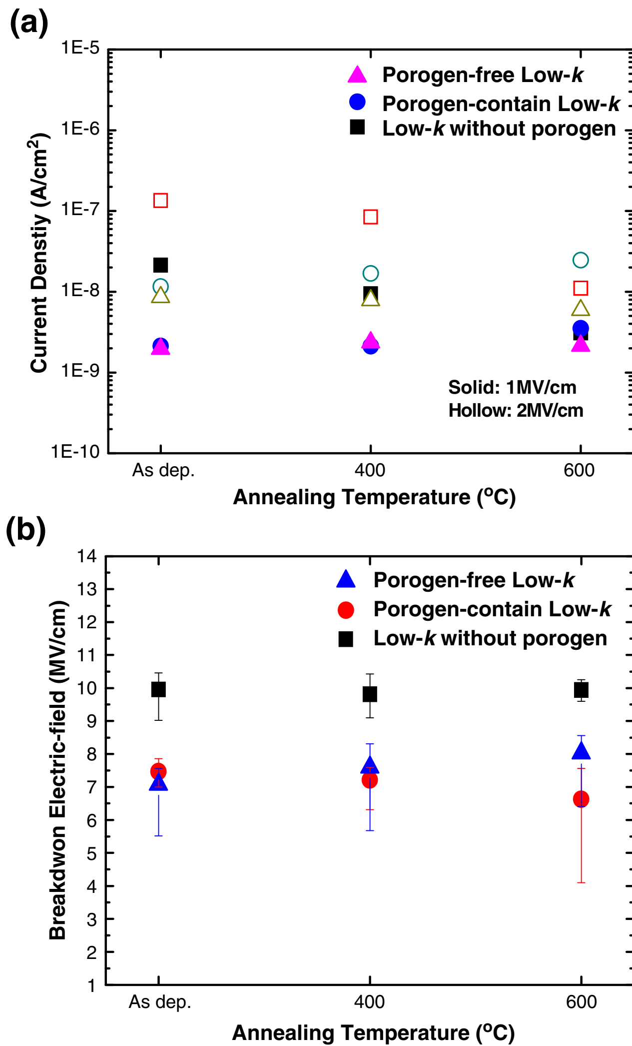

Fig. 8. (a) Leakage current density at 1 MV/cm and 2 MV/cm and (b) dielectric breakdown electric-field as functions of annealing temperature for various low-*k* films.

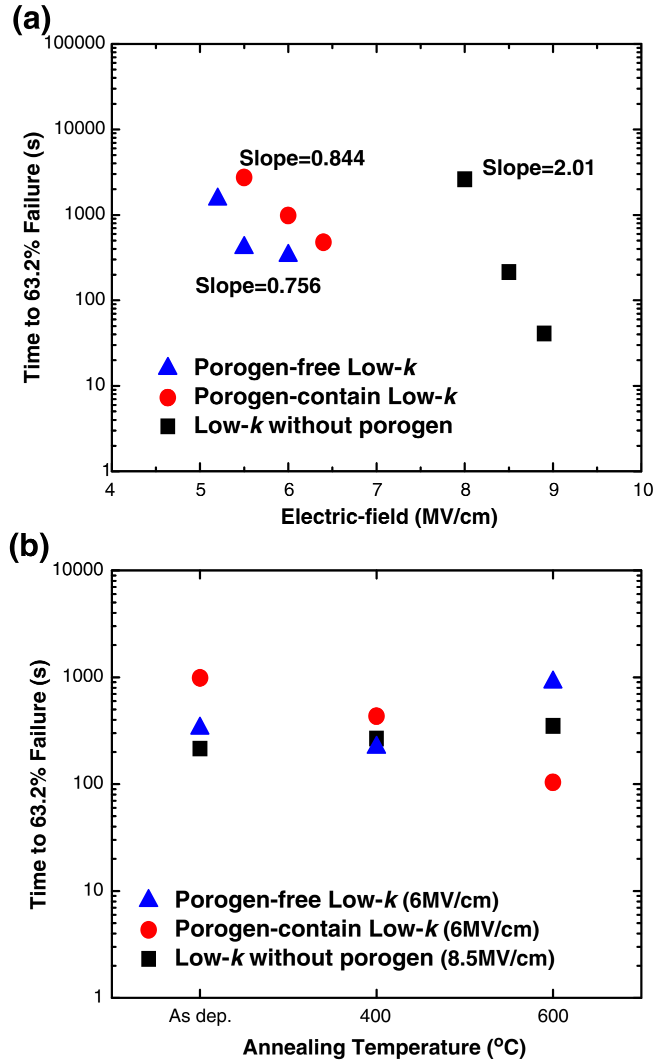

Fig. 9. (a) Time to dielectric breakdown at 63.2% failure as functions of stress electric-field for as-deposited low-*k* films and (b) time to dielectric breakdown t 63.2% failure as functions of annealing temperature for various low-*k* films.

annealing process is performed at 600 °C. This improvement is attributable to removal of porogen residues by high temperature annealing. The remaining porogen residues in the low-*k* film apparently degraded electrical performance and reliability [14].

4. Conclusions

This paper investigated the resistance of various low-*k* films against heat stress. All low-*k* films in this study were shown to be thermally stable after they were experimentally heating up to 700 °C. Additionally, non-porous low-*k* films also showed the highest reliability. Although the porous-free low-*k* film requires an additional UV curing process, the heat stress confirmed that its thermal stability was better than that of the porogen-containing low-*k* film. At an annealing temperature above 500 °C, the heating process is comparable to UV curing, but does not provide Si–O–Si cross-linking within the film. At an annealing of 600 °C, the porogen-free low-*k* films have a relatively higher breakdown electric-field and longer failure time in comparison to the porogen-containing low-*k* films. However, pores generated in porogen-containing low-*k* films at high temperature cause reliability to degrade with annealing temperature.

References

[1] A. Grill, Ann. Rev. Mater. Res. 39 (2009) 49.
[2] K. Maex, M.R. Baklanov, D. Shamiryan, F. Lacopi, S.H. Brongersma, Z.S. Yanovitskaya, J. Appl. Phys. 93 (2003) 8793.
[3] T. Furusawa, D. Ryuzaki, R. Yoneyama, Y. Homma, K. Hinode, J. Electrochem. Soc. 148 (2001) F175.
[4] A. Zenasni, B. Remiat, C. Waldfried, C.L. Cornec, V. Jousseaume, G. Passemard, Thin Solid Films 516 (2008) 1097.
[5] V. Jousseaume, O. Gourhant, P. Gonon, a. Zenasni, L. Favennec, J. Electrochem. Soc. 159 (2012) G249.
[6] F. lacopi, Y. Travaly, B. Eyckens, C. Waldfried, T. Abell, E.P. Guyer, J. Appl. Phys. 99 (2006) 053511.
[7] V. Jousseaume, A. Zenasni, L. Favennec, G. Gerbaud, M. Bardet, J.P. Simon, A. Humberte, J. Electrochem. Soc. 154 (2007) G103.
[8] A. Grill, V. Patel, J. Appl. Phys. 104 (2008) 024113.
[9] Y.W. Li, C.F. Chen, Jpn. J. Appl. Phys. 41 (2002) 5734.
[10] C.K. Choi, C.Y. Kim, R. Navamathavan, H.S. Lee, J.K. Woo, M.T. Hyun, H.J. Lee, W.Y. Jeung, Curr. Appl. Phys. 5 (2011) S109.
[11] A.M. Urbanowicz, K. Vanstreels, P. Verdonck, E.V. Besien, T. Christos, D. Shamiryan, S.D. Gendt, M.R. Baklanov, J. Vac. Sci. Technol. B29 (2011) 032201-1.
[12] E. Hong, S. Demuynck, Q.T. Le, M. Baklanov, L. Carbonell, M.V. Hove, M. Meynen, Microelectron. Eng. 84 (2007) 2582.
[13] C.H. Huang, N.F. Wang, Y.Z. Tsai, C.I. Hung, M.P. Houng, Microelectron. Eng. 87 (2010) 1735.
[14] M.R. Baklanov, L. Zhao, E.V. Besien, M. Pantouvaki, Microelectron. Eng. 88 (2011) 990.